scientific reports

Check for updates

OPEN

Natural AI-based drug designing by modification of ascorbic acid and curcumin to combat buprofezin toxicity by using molecular dynamics study

Haleema Sadia[1], Irfan Zia Qureshi[1]✉, Muhammad Naveed[2], Tariq Aziz[3]✉, Metab Alharbi[4], Abdullah F. Alasmari[4] & Thamer H. Albekairi[4]

Buprofezin, a widely employed insecticide in agricultural practices, has elicited significant apprehension due to its prospective deleterious effects on non-target organisms and ecological systems. Its enduring presence in terrestrial and aquatic environments presents potential hazards to human health and biodiversity, thereby necessitating the investigation of safer alternatives or strategies for mitigation. The research focuses on five principal receptors: CAT (Catalase), IL-1B (Interleukin-1 Beta), IL-6 (Interleukin-6), TNF-alpha (Tumor Necrosis Factor-alpha), and SOD (Superoxide Dismutase). These receptors are integral to the processes of inflammation, oxidative stress, and immune responses, rendering them critical for comprehending the biochemical pathways affected by toxic substances and the potential for protective interventions. The investigation employed WADDAICA (Webserver-Aided Drug Design by Artificial Intelligence) to formulate AI-driven pharmaceuticals, complemented by ADME (Absorption, Distribution, Metabolism, Excretion) evaluations, Molecular Dynamics (MD) simulations, as well as MMGBSA and MMPBSA methodologies to examine the stability and interactions of the compounds with the designated receptors. Docking experiments disclosed that the interaction of CAT with the ascorbic acid AI-derived drug demonstrated a binding energy of -7.1 kcal/mol, signifying a robust interaction, while the complex of IL-1B with the curcumin AI-derived drug exhibited a binding energy of -7.3 kcal/mol. The ADME analysis revealed favorable gastrointestinal absorption and aqueous solubility for both compounds. Furthermore, the drug-likeness metrics were deemed satisfactory, with no breaches of Lipinski's rule of five, suggesting promising potential for subsequent advancement as therapeutic agents.

Keywords Buprofezin, CAT (catalase), IL-1B (Interleukin-1 Beta), AI-based drug, Ascorbic acid, Curcumin

A widely utilized insecticide, renowned for its efficacy in controlling a diverse array of agricultural pests, is buprofezin. Nonetheless, its application has been associated with potentially detrimental effects on humans and various non-target organisms. It has become imperative to alleviate the toxicity attributable to buprofezin to safeguard human health and environmental integrity. The increasing reliance on synthetic pesticides, including buprofezin, has engendered significant challenges for ecological systems and human well-being. While buprofezin demonstrates considerable pest management efficiency, concerns have emerged regarding its toxicity to beneficial insect populations, soil degradation, and potential health hazards to humans upon exposure to elevated concentrations. These challenges necessitate the development of mitigation strategies that do not compromise the efficacy of pest control measures. Addressing these concerns is crucial for the preservation of public health and the advancement of sustainable agricultural practices[1].

[1]Laboratory of Animal and Human Physiology, Department of Zoology, Quaid-i-Azam University, Islamabad 45320, Pakistan. [2]Department of Biotechnology, Faculty of Science and Technology, University of Central Punjab, Lahore 54590, Pakistan. [3]Laboratory of Animal Health Food Hygiene and Quality, University of Ioannina, Arta 47132, Greece. [4]Department of Pharmacology and Toxicology College of Pharmacy, King Saud University, Riyadh, Saudi Arabia. ✉email: irfanzia@qau.edu.pk; iwockd@gmail.com

Catalase (CAT) constitutes an enzymatic protein that facilitates the decomposition of hydrogen peroxide into dihydrogen monoxide and dioxygen, thereby safeguarding cellular structures from oxidative harm[2,3]. Interleukin-1 Beta (IL-1B) constitutes a pro-inflammatory cytokine integral to the organism's immune response, thereby serving a critical function in the processes of inflammation and the induction of fever; additionally, Interleukin-6 (IL-6) represents another cytokine that facilitates immune responses, inflammatory mechanisms, and the regulation of hematopoiesis[2,3]. Tumor Necrosis Factor-alpha (TNF-alpha) serves as a pivotal modulator of inflammatory processes and programmed cell death, impacting immune system functionalities and diseases associated with chronic inflammation. Additionally, Superoxide Dismutase (SOD) functions as a crucial enzymatic catalyst that facilitates the conversion of superoxide anions into molecular oxygen and hydrogen peroxide, thereby providing a protective mechanism for cells against oxidative damage and ensuring the maintenance of cellular integrity[2,3].

Curcumin and ascorbic acid have exhibited significant potential in mitigating the detrimental effects of various chemicals and pharmacological agents. Powerful antioxidants such as ascorbic acid possess the capacity to neutralize free radicals and diminish oxidative stress induced by toxic substances like buprofezin. The primary bioactive compound in turmeric, curcumin, is endowed with antioxidant and anti-inflammatory properties that can aid in protecting cellular integrity and promoting overall well-being. The synergistic utilization of curcumin and ascorbic acid may offer a safe and natural approach to counteract the toxicity associated with buprofezin and serve as an alternative to conventional pesticides[4].

Buprofezin, widely used as an insect growth regulator, has been linked to oxidative stress and inflammation in non-target organisms. This leads to cellular damage by increasing reactive oxygen species (ROS), which directly affects the receptors in question. Catalase (CAT) is responsible for deactivating hydrogen peroxide, a major ROS, and its depletion due to Buprofezin can cause further oxidative damage[5,6]. Superoxide Dismutase (SOD) plays a similar protective role by converting superoxide radicals into less harmful molecules. Inflammatory cytokines like IL-1B, IL-6, and TNF-alpha are also involved, with Buprofezin promoting their expression, exacerbating inflammatory responses, and potentially triggering apoptosis[5,6]. Ascorbic Acid and Curcumin are specifically chosen for their antioxidant and anti-inflammatory properties, countering these effects by enhancing CAT and SOD activity and reducing the levels of IL-1B, IL-6, and TNF-alpha. Ascorbic Acid scavenges free radicals and supports enzymatic antioxidants, while Curcumin inhibits pro-inflammatory cytokines and boosts antioxidant defenses, making them effective in reducing Buprofezin-induced damage[5,6].

AI-driven pharmaceuticals epitomize a revolutionary paradigm in pharmacological research, employing artificial intelligence to devise and refine molecular entities exhibiting therapeutic efficacy. Through the application of AI methodologies, investigators are able to swiftly produce and evaluate extensive collections of compounds, discerning those with the greatest propensity for effective binding to designated receptors[7]. These methodologies, propelled by artificial intelligence, not only augment the efficacy of pharmaceutical design but also elevate the precision of forecasting molecular interactions, pharmacokinetic behaviors, and toxicity characteristics[8]. The utilization of artificial intelligence in pharmacological development significantly expedites the identification of innovative therapeutic interventions, diminishes associated expenditures, and creates unprecedented opportunities for tailored medical approaches, thereby establishing itself as an instrumental resource in the battle against intricate diseases[9]. The principal objective of this investigation is to formulate a pioneering pharmacophore-based therapeutic agent enhanced by artificial intelligence, aimed at effectively mitigating the toxicity associated with buprofezin. By employing artificial intelligence methodologies, researchers are able to identify novel compounds that may alleviate the harmful effects of buprofezin while simultaneously maintaining its pest management efficacy. The utilization of AI in pharmaceutical development optimizes the exploration for safe and effective molecular entities by facilitating the rapid assessment of extensive chemical libraries[7].

The incorporation of artificial intelligence in pharmacophore modeling has the potential to enhance both the precision and efficiency of pharmaceutical development. Artificial intelligence systems possess the capability to identify critical molecular interactions, predict the biological efficacy of potential compounds, and refine therapeutic candidates to optimize their safety and effectiveness. This approach promotes safer agricultural methodologies and improved public health results by accelerating the pharmaceutical development timeline and providing a robust framework for the formulation of targeted strategies aimed at mitigating Buprofezin-induced toxicity.

Methods

Sequence retrieval of the receptor proteins

The FASTA format sequences of the receptor proteins were retrieved from the NCBI protein database (https://www.ncbi.nlm.nih.gov/)[10]. The accession numbers and corresponding names of the retrieved proteins are provided in Table 1.

Receptor protein 3D structure retrieval

Using Swiss-Model, the 3D structures of the receptor proteins were modelled. (https://swissmodel.expasy.org/)[11]. The model with the highest identity and coverage was chosen based on the FASTA sequences of the receptor proteins.

Receptor protein 3D structure validation

Making sure the protein 3D structures were accurate was a crucial step in guaranteeing the correctness of the docking and molecular modeling processes. For this, the Ramachandran plot and ERRAT were used, which offered complementary information regarding the accuracy of the protein structures that were modeled (https://www.doe-mbi.ucla.edu/errat/)[12,13].

Sr.	Receptor proteins	Accession numbers
1.	CAT (catalase)	NP_001743.1
2.	IL-1B (interleukin 1 beta)	NP_000567.1
3.	IL-6 (interleukin 6)	XP_054214120.1
4.	TNF- α (tumor necrosis factor alpha)	NP_000585.2
5.	SOD (superoxide dismutase)	AAR21563.1

Table 1. Accession no. of receptor proteins FASTA formats.

	Size			Center		
Receptors	X	Y	Z	X	Y	Z
CAT	35.24	33.42	39.47	− 5.36	2.06	− 0.91
IL-1B	27.55	30.63	39.47	− 1.5	10.41	− 11.46
IL-6	26.76	30.63	34.32	1.66	2.19	− 1.83
SOD	26.76	3.69	− 0.12	26.76	25.01	18.75
TNF-alpha	20.93	24.48	33.1	− 3.63	2.1	− 6.68

Table 2. Grid box settings of all receptors.

Plotting the φ (phi) and ψ (psi) angles on a two-dimensional plane allowed for the evaluation of the torsion angles of the amino acid residues in the protein using the Ramachandran plot. This study is important because it confirms the protein's structural integrity by pointing out residues that are in conformations that are energetically advantageous. A well-modeled protein is indicated by residues that lie inside the Ramachandran plot's permitted regions; deviations may point to structurally problematic regions.

ERRAT was utilized to find possible chain breaks, mistakes, and warnings in the PDB files in order to evaluate the overall quality of the protein model. By examining the non-bonded atomic interactions, ERRAT is able to identify areas where the protein structure may be jeopardized or the model may not be accurate. To make sure the protein model is appropriate for later docking and molecular interaction research, this validation step is crucial. By reducing the possibility of docking process errors and improving the accuracy of the projected ligand-receptor interactions, these validation methods aid in ensuring that the protein models utilized in drug design were of the highest caliber.

Ascorbic acid and curcumin structure retrieval

The 3D structures of ascorbic acid and curcumin were retrieved from the PubChem database (https://pubchem.ncbi.nlm.nih.gov/), with the PubChem CID for ascorbic acid being 54,670,067 and for curcumin being 969,516. The SDF and SMILES formats of both ligands were used for further analysis[14].

AI drug modeling and pharmacophore characterization

WADDAICA (Webserver-Aided Drug Design by Artificial Intelligence and Classical Algorithm) was employed to generate six drug candidates for each ligand https://heisenberg.ucam.edu:5000/[9,15]. This AI-based tool enhances the pharmacophore of existing drugs using the SMILES format. The SMILES formats of both ligands were input into WADDAICA, resulting in the creation of six AI-designed ligands.

The pharmacophore characterization of these AI ligands was then performed using the Pharmit server (https://pharmit.csb.pitt.edu/)[16,17]. The Mol formats of the AI ligands were provided to Pharmit, which analyzed and identified their pharmacophore properties, including hydrogen bond donors or acceptors, aromatic rings, ion donors, and hydrophobic regions.

Virtual screening of AI ligands

The virtual screening of the AI ligands was conducted for each receptor using PyRx[18,19]. PyRx is a widely used suite for docking screening, based on the AutoDock Vina algorithm. The screening process was based on the binding affinity energies of the ligands. Initially, the receptor proteins were converted into PDBQT files. Following this, the AI ligands were uploaded, and their energies were minimized. After energy minimization, the AI ligands were also converted into PDBQT files. PyRx was then configured to perform Molecular Dynamics (MD) docking, with a grid box set for each receptor. The specific grid box settings for each receptor are detailed in the Table 2. To validate the docking results CB Dock 2 based on vina docking that performed blind docking of the ligands was used[20].

Molecular interactions

Molecular interactions between drug candidates and their target receptors play a critical role in determining the efficacy and specificity of the therapeutic agent. To ensure that the AI-generated ligands effectively bind to their respective receptors, the molecular interactions of the best docked complexes were meticulously analyzed. For

this purpose, Discovery Studio, PLIP (Protein-Ligand Interaction Profiler) (https://plip-tool.biotec.tu-dresden.de/plip-web/plip/index), and PyMOL were utilized[21,22].

Analyzing these interactions was essential for determining the binding affinity, which directly correlates with the potential efficacy of the drug candidate. Moreover, understanding the nature and strength of these interactions aids in the optimization of the ligand structure, ensuring that the designed molecules exhibit the desired pharmacological activity while minimizing off-target effects. This step was crucial in advancing promising candidates through the drug development.

Molecular dynamics simulations

The AMBER suite of programs was utilized to perform molecular dynamics (MD) simulations in order to examine the dynamic behavior of two docked complexes: IL-1B with AI ligand 3 and CAT protein with ascorbic acid AI ligand 1. For the protein, the AMBER ff19SB force field was employed, and for the ligand structures, the General AMBER Force Field 2 (GAFF2) was used[23]. In a TIP3P water model, both complexes were solvated using a simulation box that extended 12 Å in all directions from the solute[24]. In order to neutralize the system and simulate physiological circumstances, sodium and chloride ions (NaCl) were supplied. After 20,000 steps of energy minimization to eliminate any steric conflicts or unfavorable interactions, the systems were allowed to equilibrate for 5 nanoseconds at a constant temperature (298 K) and pressure (1 bar) using an integration timestep of 2 femtoseconds (fs). The same pressure and temperature conditions were used for the production MD simulations, and 2,000 frames of trajectory data were obtained every 10 picoseconds. Following simulation, the complexes' binding free energies were determined using the Molecular Mechanics Generalized Born Surface Area (MMGBSA) and MMPBSA methods[25,26]. With the use of this combination method, it was possible to thoroughly analyze the complexes' structural stability and interaction patterns in a watery environment, providing important new information about their potential as medicinal agents.

Pre-clinical testing (ADMET)

In drug design, assessing key pharmacokinetic properties is crucial to ensure that the AI-generated ligands possess favorable characteristics for therapeutic use. SwissADME (http://www.swissadme.ch/index.php) was used to evaluate the ligands for Total Polar Surface Area (TPSA), Lipophilicity, water solubility, Blood-Brain Barrier (BBB) penetration, Gastrointestinal (GI) absorption, and Drug-likeness. These factors are critical because they affect the drug candidates' absorption, distribution, metabolism, and excretion (ADME)[3]. When forecasting a molecule's capacity to cross cell membranes and affect both GI absorption and BBB penetration, TPSA is important. The molecule's permeability and solubility are influenced by lipophilicity; an ideal balance is required for effective absorption and interaction with biological targets. The drug's water solubility affects its distribution to the site of action by determining its bioavailability and simplicity of formulation. Drugs aimed at the central nervous system must penetrate the blood-brain barrier (BBB) since this demonstrates the molecule's capacity to enter the brain. Oral bioavailability, or the capacity of the medication to be efficiently absorbed when taken orally, depends on GI absorption. Drug-likeness assesses how closely a molecule resembles well-known medications and forecasts how well it will work as a therapeutic agent. Toxicity is an important factor for the determination of the lead drugs candidates in pre-clinical trials. The toxicity of the lead drug candidates was predicted by Deep-pk (deep learning for small molecule pharmacokinetic and toxicity prediction) server[27].

Results

Receptor protein 3D structures

The 3D structures of the receptor proteins, including the CAT protein which was modeled, were retrieved from AlphaFold and are illustrated in Fig. 1. The PDB models with the highest identity and coverage were selected for further analysis. The identity and coverage values for these models are provided in the Table 3.

Receptor protein 3D structure validation

The quality of the 3D structures of the receptor proteins was assessed using the Ramachandran plot, which is illustrated in Fig. 2. This plot was used to evaluate the conformational angles of the amino acid residues and ensure the structural integrity of the proteins. Additionally, ERRAT was employed to examine the 3D structures for potential chain breaks and warnings, with the resulting ERRAT graphs shown in Fig. 3. The detailed values from the Ramachandran plot and ERRAT analysis are provided in the Table 4.

Ascorbic acid and curcumin structure retrieval

The 3D structures of ascorbic acid and curcumin, as retrieved from PubChem, are depicted in Fig. 4. The SMILES formats for both ligands are provided in the Table 5.

AI ligands modeling and characterization

Six AI-designed ligands were generated for each of the original ligands. The details of the AI ligands for ascorbic acid and curcumin are provided in Table 6. The pharmacophore properties of these AI ligands are illustrated in Figs. 5 and 6.

Virtual screening of AI ligands

The highest binding affinity for the ascorbic acid AI ligands was observed with the catalase (CAT) protein, exhibiting a binding affinity of -7.1 kJ/mol. For the curcumin AI ligands, the highest binding affinity was with the IL-1β (Interleukin 1 beta) protein, showing a binding affinity of -7.3 kJ/mol. The binding affinities of all AI ligands with their respective receptor proteins are detailed in Table 7.

Among the ascorbic acid AI ligands, the highest binding affinities were:

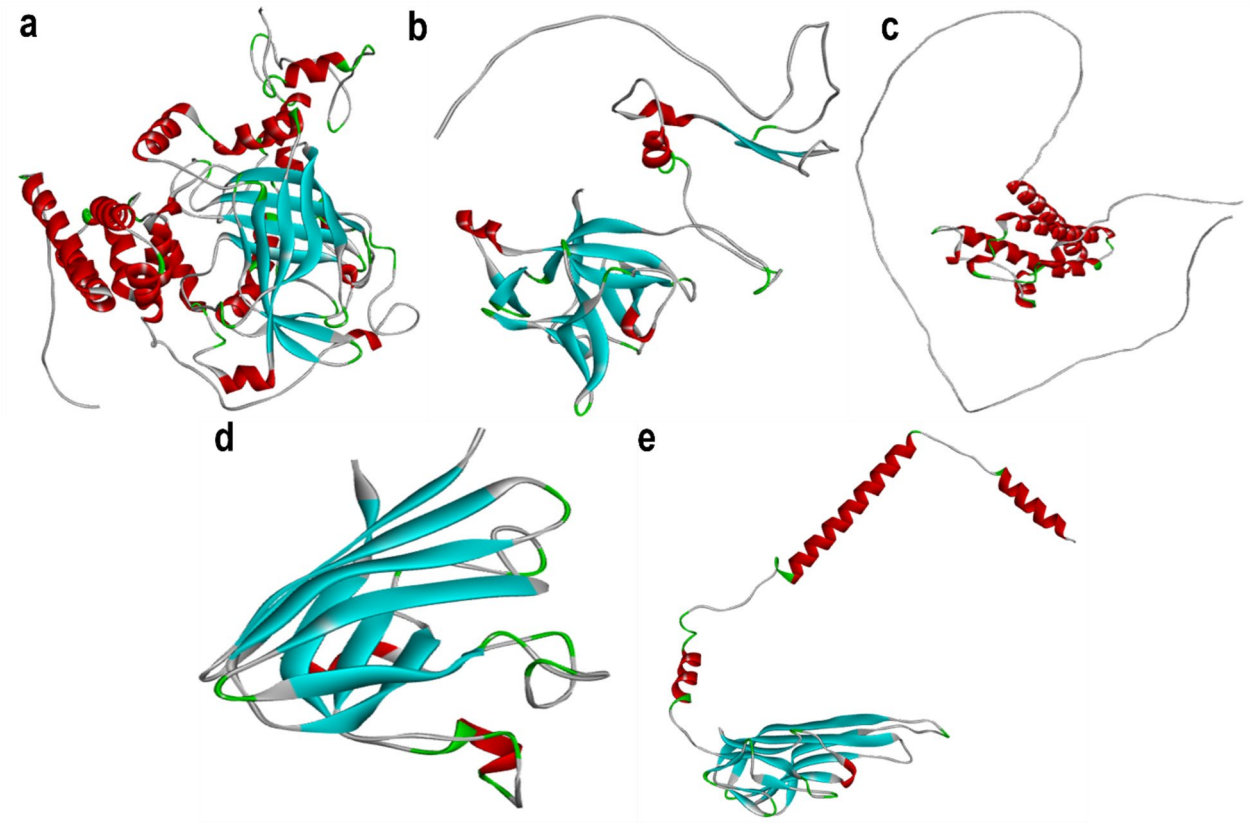

Fig. 1. 3D structure of receptors protein (**a**) CAT form AlphaFold (**b**) IL-1B form Swiss-model (**c**) IL-6 form Swiss-model (**d**) SOD form Swiss-model (**e**) TNF- α form Swiss-model.

Sr.	Receptor proteins	Identity	Coverage quality
1.	Catalase (CAT)	91.97%	Excellent
2.	IL-1B (interleukin 1 beta)	90.71%	Excellent
3.	IL-6 (interleukin 6)	95.63%	Excellent
4.	SOD (superoxide dismutase)	82.78%	Excellent
5.	TNF- α (tumor necrosis factor alpha)	94.85%	Excellent

Table 3. The identity and coverage of model protein 3D receptors.

1. IL-1β with ligand 6: -6.6 kJ/mol.
2. IL-6 with ligand 3: -6.6 kJ/mol.
3. SOD with ligand 3: -5.6 kJ/mol.
4. TNF-α with ligands 3 and 6: -5.9 kJ/mol.

For the curcumin AI ligands, the highest binding affinities were:

1. CAT with ligand 2: -6.5 kJ/mol.
2. IL-6 with ligand 3: -6.8 kJ/mol.
3. SOD with ligand 2: -6.5 kJ/mol.
4. TNF-α with ligands 1 and 2: -5.9 kJ/mol.

Molecular interactions

The molecular interactions of the top AI ligands with each receptor protein were analyzed. Figure 7 illustrates the interactions of the ascorbic acid AI ligands with the receptor proteins, while Fig. 8 shows the interactions of the curcumin AI ligands with the receptor proteins. Detailed information on the molecular interactions of the top docked complexes—ascorbic acid AI ligand 1 with CAT and curcumin AI ligand 3 with IL-1β—can be found in the Table 8.

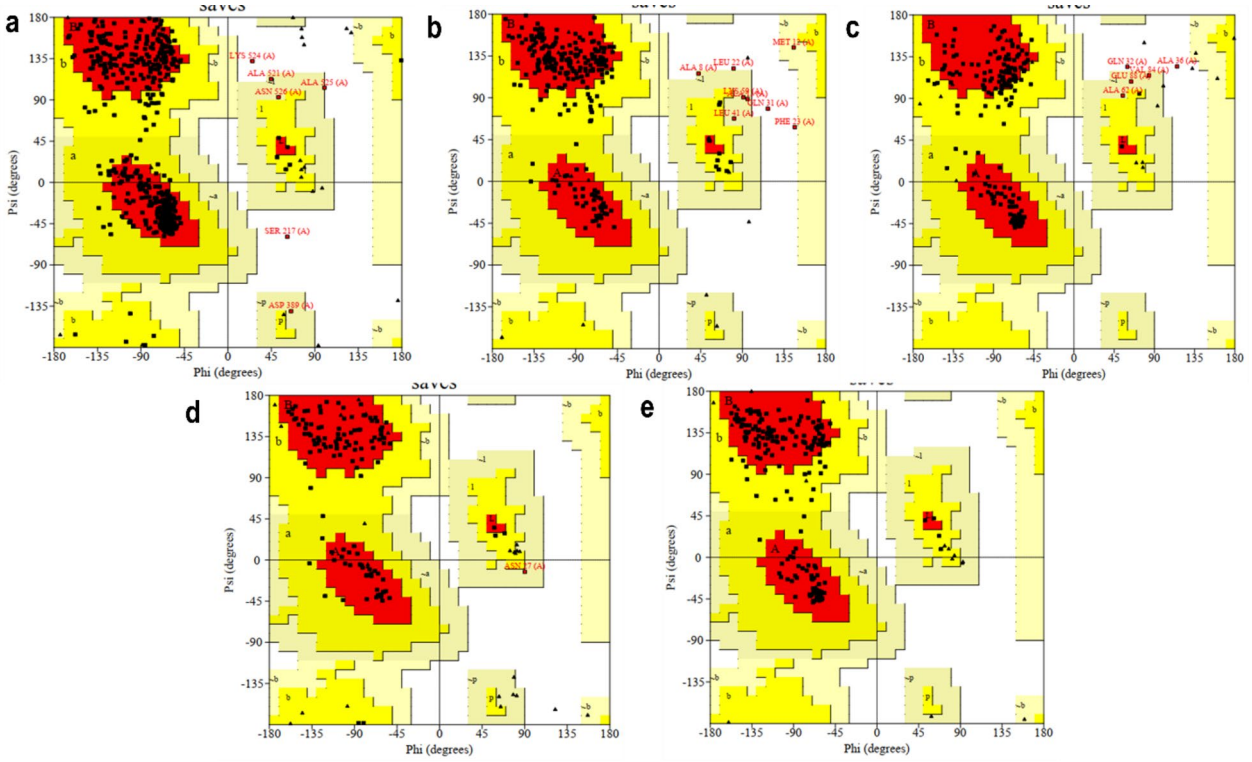

Fig. 2. Ramachandran plots of receptor protein 3D structures. (**a**) CAT (Catalase), (**b**) IL-1B (Interleukin 1 beta), (**c**) IL-6 (Interleukin 6), (**d**) TNF- α (Tumor necrosis factor alpha) and (**e**) SOD (Superoxide dismutase). The Red highlighted regions are the most favored regions, Yellow highlighted regions are additional allowed regions, Light Yellow highlighted regions is generously allowed regions, White highlighted regions are disallowed regions.

Molecular dynamics simulations, MMGBSA and MMPBSA

The molecular dynamics simulations assessed two different protein-ligand complexes: CAT with Ascorbic acid AI ligand 1, and IL-1B with curcumin AI ligand 3. Both complexes were analyzed based Root Mean Square Deviation (RMSD), Root Mean Square Fluctuation (RMSF), and Radius of Gyration (Rg).

Comparing the two complexes, both CAT and IL-1B showed overall stability during the simulations, but with different degrees of flexibility and structural adjustments. The RMSD for the IL-1B complex indicated fewer fluctuations, suggesting a more stable binding compared to CAT. However, both complexes exhibited stable Rg values, demonstrating that neither interaction significantly disrupted the protein's compactness. The RMSF analysis further supports this, as both complexes showed flexibility in specific regions but stabilized over time.

The energy profiles for both complexes remained stable throughout the simulation. For CAT with Ascorbic acid AI ligand 1, the highest energy interactions were observed at -7521 kCal/mol after 78 nanoseconds, indicating stable binding Fig. 12a. The IL-1B-curcumin AI ligand 3 complex, was expected to exhibit similarly stable energy values, given its consistent structural stability across other parameters Fig. 12b.

The principal component analysis (PCA) was conducted to study the major conformational changes during molecular dynamics (MD) simulations of two protein-ligand complexes: CAT protein with ascorbic acid AI ligand 1, and IL-1B protein with curcumin AI ligand 3. For both complexes, the first two principal components (PC1 and PC2) were analyzed, representing the primary modes of motion within the protein-ligand interactions. In the CAT-ascorbic acid complex, PC1 show for the largest variance, indicating the primary conformational shifts, while PC2 captured secondary changes, revealing significant fluctuations and suggesting that the CAT protein experiences notable conformational flexibility when bound to the ascorbic acid ligand Fig. 13a. The IL-1B-curcumin complex, PC1 and PC2 described substantial fluctuations, reflecting a dynamic interaction and suggesting that the IL-1B protein shows various conformational states stabilized by curcumin Fig. 13b. Both complexes demonstrate a high degree of conformational variability and the dynamic nature of the protein-ligand interactions, which are improtant in modulating the proteins functional efficacy and stability. Especially, the extent of conformational changes was similar in both complexes, suggesting that both ligands induce significant flexibility in their respective protein targets, potentially enhancing their therapeutic potential.

The results of the MMGBSA and MMPBSA analyses for the CAT (Catalase) and IL-1B complexes with ascorbic acid AI Ligand 1 and curcumin AI Ligand 3 demonstrate that both ligands exhibit favorable binding energies, indicating stable interactions within the receptor's binding pocket.

For the CAT ascorbic acid AI Ligand 1 complex, the MMGBSA analysis shows a total binding free energy (ΔG total) of -19.7907 kcal/mol, while the MMPBSA analysis yields a slightly positive total binding energy

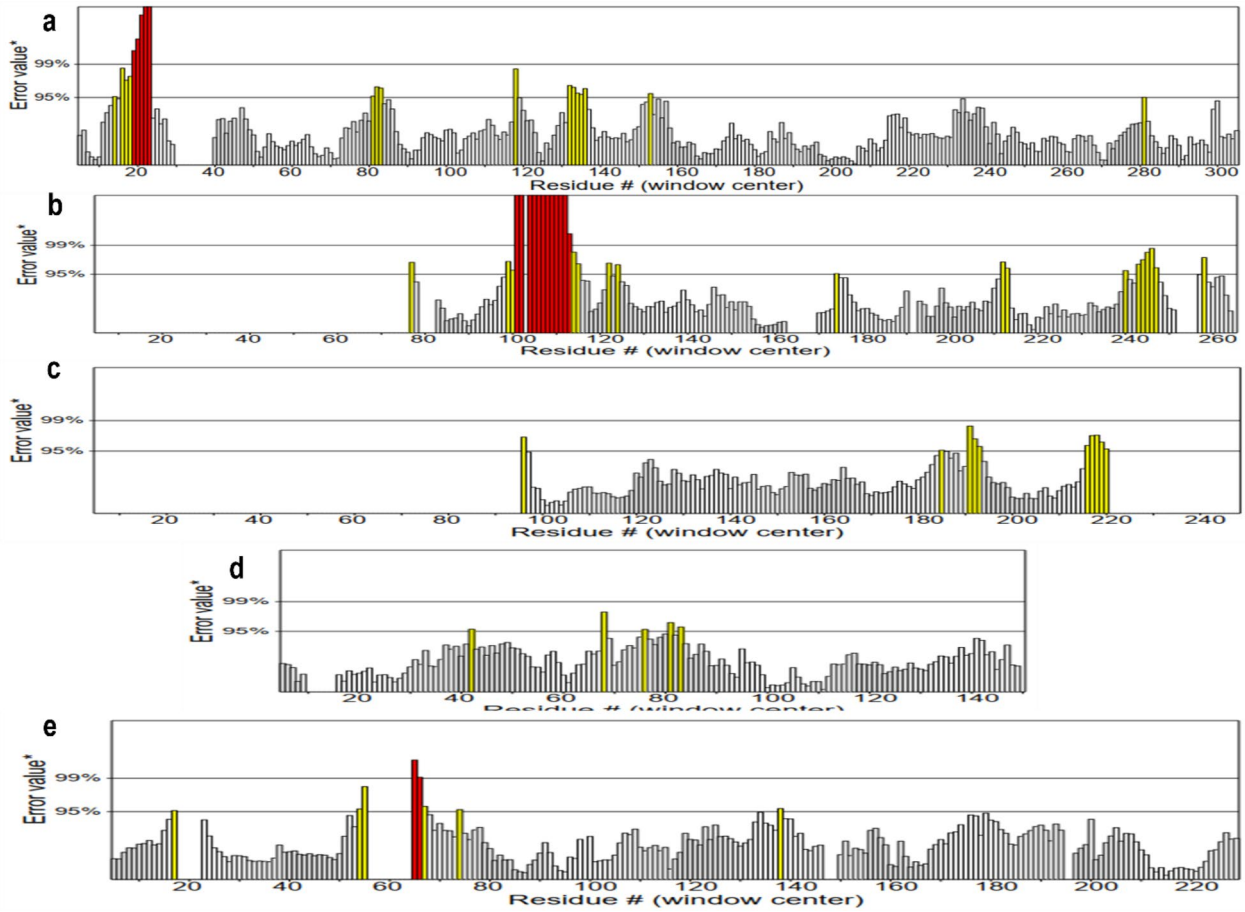

Fig. 3. ERRAT Graphs of receptor proteins 3D structures (**a**) Catalase (CAT) CAT, (**b**) IL-1B (Interleukin 1 beta), (**c**) IL-6 (Interleukin 6) (**d**) SOD (Superoxide dismutase) and (**e**) TNF-α (Tumor necrosis factor alpha). The red lines are error and the yellow lines are the warnings.

Sr.	Receptor proteins	Most favored regions	Additional allowed regions	Generously allowed regions	Disallowed regions	ERRAT score
1.	CAT (catalase)	87.0%	11.7%	0.9%	0.4%	94.167
2.	IL-1B (interleukin 1 beta)	83.7%	13.0%	2.1%	1.3%	82.840
3.	IL-6 (interleukin 6)	85.3%	12.4%	1.4%	0.9%	92.000
4.	TNF-α (tumor necrosis factor alpha)	89.4%	10.6%	0.0%	0.0%	96.078
5.	SOD (superoxide dismutase)	89.3%	9.8%	0.8%	0.0%	96.403

Table 4. Ramachandran plot and ERRAT values of receptor proteins 3D structures.

(ΔG total) of -0.7140 kcal/mol Tables 9 and 10. The significant negative energy from MMGBSA and MMPBSA analysis confirms that the ligand fits well into the binding pocket and forms a stable complex with CAT.

The IL-1B curcumin AI Ligand 3 complex shows a strong binding affinity, with the MMGBSA analysis yielding a ΔG total of -37.2074 kcal/mol, and the MMPBSA analysis showing a slightly positive ΔG total of 1.0696 kcal/mol Tables 11 and 12. The substantial negative energy from the MMGBSA and MMPBSA analysis suggests that ligand also binds effectively to IL-1B, with the ligand fitting well into the receptor's binding pocket.

Both AI Ligand 1 and AI Ligand 3 form stable complexes with CAT and IL-1B, as indicated by the negative binding energies from the MMGBSA analyses. The MMGBSA and MMPBSA results collectively suggest that the ligands are properly accommodated within the receptor, supporting their potential as effective inhibitors or modulators of CAT activity.

Pre-clinical testing (ADMET)

The ADME properties of the ascorbic acid AI ligands were found to be excellent, making them promising candidates for lead drug development. The TPSA and lipophilicity values were within the optimal range, indicating good solubility and high gastrointestinal (GI) absorption. None of the AI ligands violated Lipinski's rule, suggesting favorable drug-likeness. Similarly, the ADME properties of the curcumin AI ligands were also

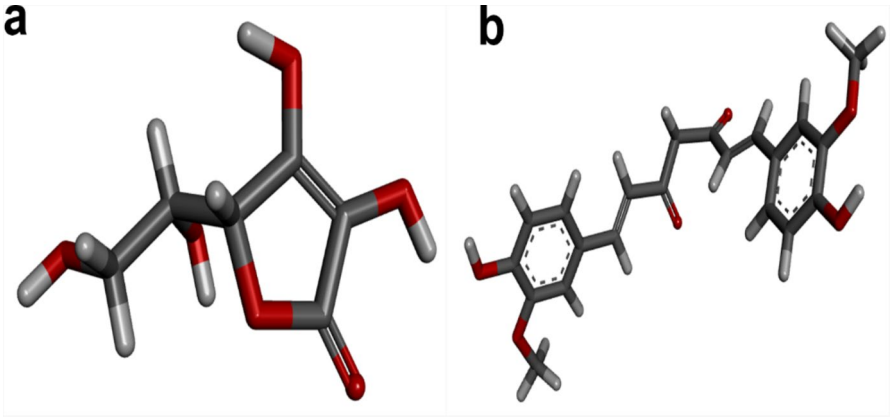

Fig. 4. (**a**) 3D structures of Ascorbic acid and (**b**) 3D structures of Curcumin.

Sr.	Ligands	Smiles
1.	Ascorbic acid	C([C@@H]([C@@H]1 C(=C(C(=O)O1)O)O)O)O
2.	Curcumin	COC1=C(C=CC(=C1)/C=C/C(=O)CC(=O)/C=C/C2=CC(=C(C=C2)O)OC)O

Table 5. Smiles format of ascorbic acid and curcumin retrieved from NCBI PubChem.

favorable for lead drug candidates. The TPSA and lipophilicity values indicated moderate solubility, high GI absorption, and the potential for blood- brain barrier (BBB) crossing. None of the AI ligands violated Lipinski's rule, reflecting good drug-likeness. Detailed ADME properties for both ascorbic acid and curcumin AI ligands are provided in Table 13. The Boiled Egg diagrams for the ascorbic acid and curcumin AI ligands are shown in Fig. 14.

The Ascorbic acid AI lead drug candidate show low toxicity and it is a safe compound and have passed all filters of toxicity except Bee, Biodegradation, Eye irritation, Liver Injury II, Micronucleos with normal range of confidence score. Although the Liver Injury II have a low confidence score and it may or may not show liver toxicity in the body. These Parameter show some toxicity in the AI lead drug of ascorbic acid (Table 14). The Curcumin show medium level of toxicity but the main parameters of toxicity show that curcumin was safe. The parameter that showed toxicity were Bee, Crustacean, Liver Injury I, Liver Injury II, hERG Blockers, Micronucleos, NR-AhR, NR-GR, SR-ARE, and SR-MMP from which the main toxicity parameters Liver Injury I and Liver Injury II shows low confidence score as compare to others. These results predict that Curcumin AI lead compound can also be a good lead drug candidate in preclinical trails (Table 14).

Discussion

It has been demonstrated that the common insecticide buprofezin causes considerable oxidative stress and inflammation in non-target creatures, such as humans. By inhibiting the manufacture of chitin, it prevents pests from growing, but it also creates reactive oxygen species (ROS) and starts inflammatory processes that can be harmful to cells. Previous research has shown the negative impacts of exposure to buprofezin, emphasizing the necessity for measures to lessen its detrimental effects[28].

Turmeric's bioactive ingredient, curcumin, has shown strong anti-inflammatory and antioxidant qualities, making it a strong contender to mitigate buprofezin's toxicity. The literature has provided ample evidence of curcumin's capacity to neutralize ROS and modify important signaling pathways connected to inflammation and apoptosis[29]. Similarly, by scavenging free radicals and reestablishing the equilibrium of antioxidants, vitamin C, an essential antioxidant, protects cells from oxidative damage. It has been proposed that vitamin C and curcumin work in concert to provide increased protection against inflammation and oxidative stress[30].

Curcumin, derived from *Curcuma longa*, has shown potent antioxidant activities by inhibiting ROS production and reducing inflammatory responses. Its ability to suppress pro-inflammatory cytokines, such as IL-1β and TNF-α, highlights its therapeutic potential in inflammation and cancer therapy[6]. However, a significant limitation in its clinical application is its poor bioavailability in humans, which reduces its efficacy despite strong in vitro results[31,32]. Strategies like combining curcumin with bioavailability enhancers or developing novel delivery systems may help overcome this challenge[31,32]. Ascorbic acid (vitamin C) is another powerful antioxidant that neutralizes free radicals and reduces oxidative damage[33]. It supports cellular health by regenerating other antioxidants and preventing lipid peroxidation. Ascorbic acid's role in scavenging reactive oxygen species (ROS) makes it a vital agent in reducing inflammation, particularly in oxidative stress-related conditions such as cardiovascular diseases and cancer[34]. Recent studies have also explored its combination with other antioxidants, such as curcumin, to enhance therapeutic effects[32].

In-silico approaches to explore the protective potential of curcumin and vitamin C against buprofezin-induced toxicity. Three-dimensional (3D) models of receptor proteins related to inflammation and oxidative

No.	Smiles	3D structures
Ascorbic acid		
1.	O=C(O)C1CC(F)CN1C(=O)C(=O)O	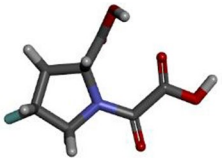
2.	O=C(O)C1CC(F)CN1C(=O)C(O)CO	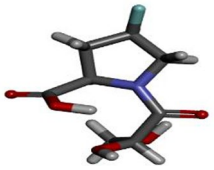
3.	O=C(O)C1CC(F)CN1C(=O)C(O)c1cccc(F)c1	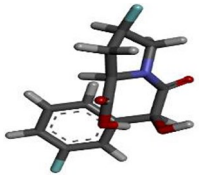
4.	O=C(O)C1CC(F)CN1C(=O)O	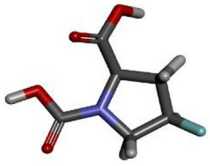
5.	O=C(O)C1COCCN1C(=O)C(=O)O	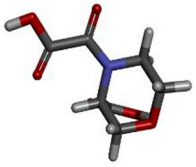
6.	O=C(O)C1CC(F)CN1C(=O)CO	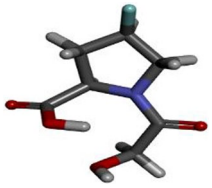
Curcumin		
1.	COc1ccc(CCCCC(=O)N2CC(C(=O)O)c3cc(F)ccc32)cc1OC	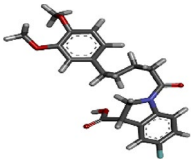
2.	COc1cc(C=CC(=O)CCC(=O)Nc2ccc3c(c2)OCCO3)ccc1OC(F)F	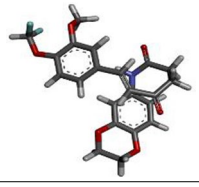
3.	COc1ccc(CCCCCC(=O)N2CC(=O)Nc3cc(OC)ccc32)cc1OC	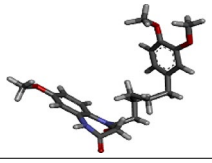
Continued		

No.	Smiles	3D structures
4.	COc1cc(CCC(=O)OCCCCOc2ccc(C)c(F)c2)cc(OC)c1	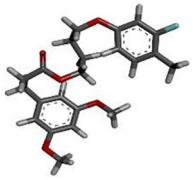
5.	COc1cc(CCC(=O)OCCCCc2ccc(OC)cc2)cc(OC)c1O	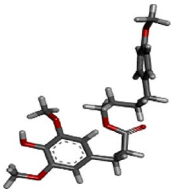
6.	COc1cc(CCC(=O)NCCCCOc2ccc(F)cc2)cc(OC)c1OC	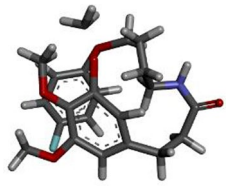

Table 6. AI ligands details of ascorbic acid and curcumin.

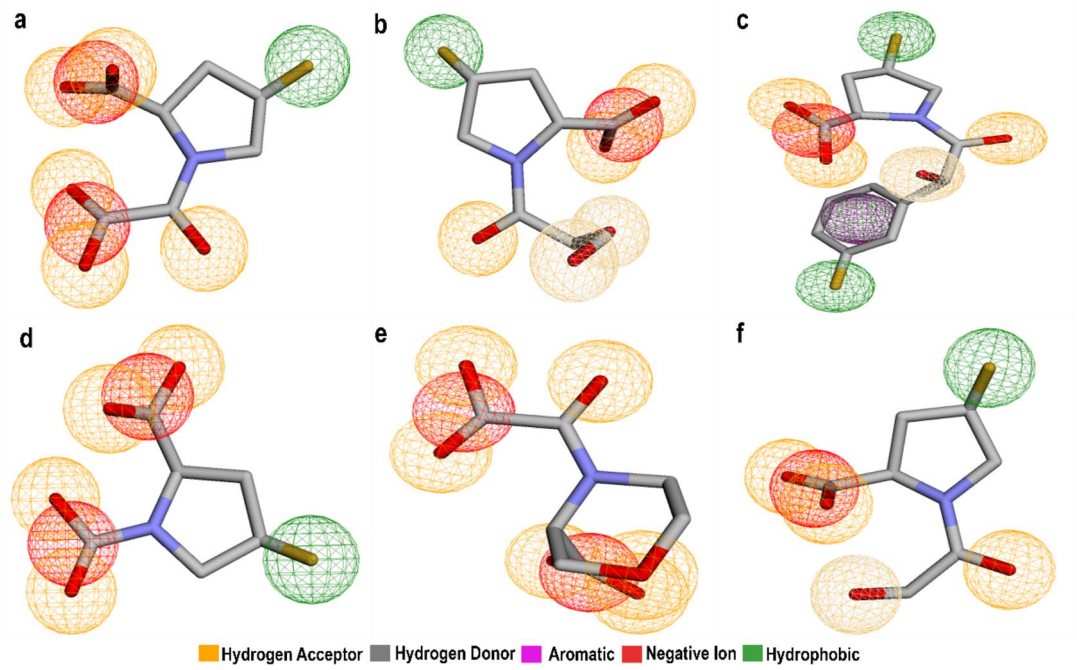

Fig. 5. Pharmacophore properties of ascorbic acid AI ligands (**a**) AI ligand no.1 (**b**) AI ligand no. 2 (**c**) AI ligand no. 3 (**d**) AI ligand no. 4 (**e**) AI ligand no. 5 (**f**) AI ligand no. 6. The yellow circles are hydrogen acceptor regions, the grey circles are hydrogen donor regions, the purple circles are aromatic regions, the red circles are negative ion regions and the green circles are hydrophobic regions.

stress, including superoxide dismutase (SOD), catalase (CAT), interleukin-1 beta (IL-1B), interleukin-6 (IL-6), and tumor necrosis factor-alpha (TNF-α), was modeled using the Swiss Model. The validity of these models was confirmed through strong sequence identity and coverage, enabling further examination.

Molecular docking studies revealed significant interactions between the AI ligands (curcumin, vitamin C, and buprofezin) and the target proteins, suggesting possible protective effects. Curcumin AI ligand have a strong binding affinity to IL-6, showing its potential to block pro-inflammatory cytokines and reduce inflammation, while vitamin C AI ligand shows moderate binding to CAT, a key enzyme in the antioxidant defense system.

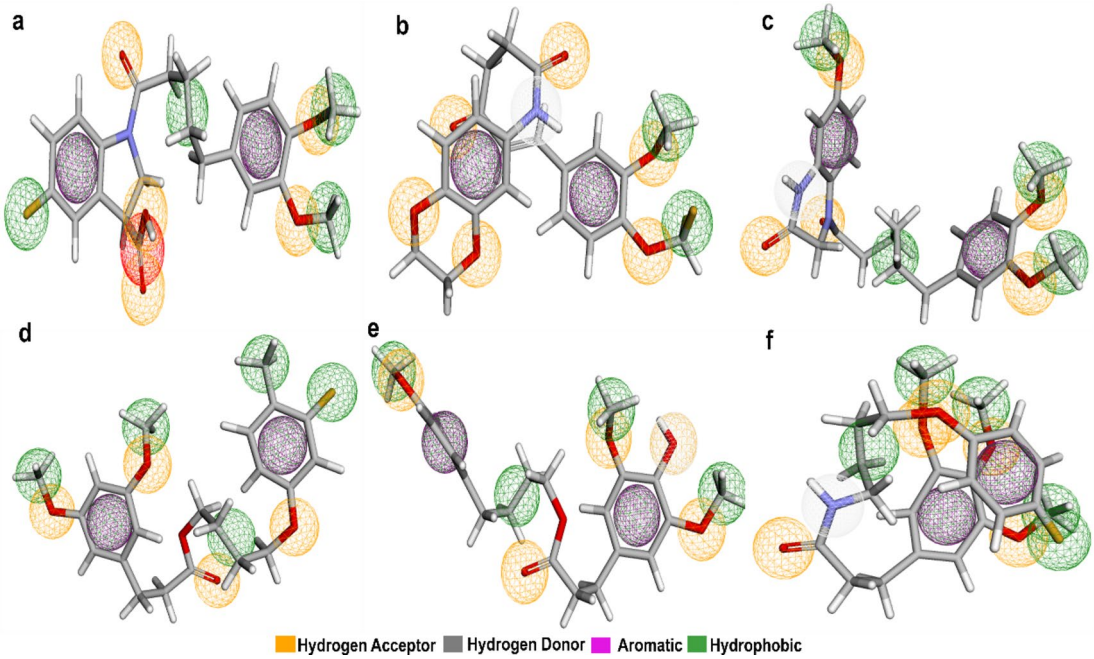

Fig. 6. Pharmacophore properties of curcumin AI ligands (**a**) AI ligand no.1 (**b**) AI ligand no. 2 (**c**) AI ligand no. 3 (**d**) AI ligand no. 4 (**e**) AI ligand no. 5 (**f**) AI ligand no. 6. The yellow circles are hydrogen acceptor regions, the grey circles are hydrogen donor regions, the purple circles are aromatic regions, and the green circles are hydrophobic regions.

These findings imply that vitamin C AI ligand could enhance cellular antioxidant capacity, mitigating the oxidative stress induced by buprofezin.

When compared to previous studies, such as the work on pharmacophore design for Philadelphia Chromosome-Positive Leukemia using Gamma-Tocotrienol, our findings align in representing the efficacy of computational methods in identifying therapeutic potential[9]. Just as the referenced study utilized in silico approaches for toxicity comparison in leukemia, our research shows how curcumin AI ligand and vitamin C AI ligand, with their favorable ADME profiles and strong binding affinities, can be considered effective agents against pesticide-induced toxicity[9]. Moreover, the role of AI and computational tools in your study parallels the methodology used in developing antimicrobial drug molecules to combat drug-resistant infections, further highlighting the versatility of AI in drug discovery[35].

Molecular dynamics simulations also reflect the findings in cancer precision drug discovery studies, where the stability of protein-ligand complexes is crucial. The stable energy profiles and conformational stability observed in our CAT-Ascorbic acid AI ligand and IL-1B-curcumin AI ligand complexes strengthen the idea that computational biology can reliably predict therapeutic efficacy, not only in oncology but also in addressing toxicity from environmental pollutants like buprofezin[35].

ADMET analysis and molecular docking experiments indicate that curcumin and vitamin C AI ligand may be useful therapies to combat buprofezin's negative effects having minimum toxicity. Compared to buprofezin, these compounds had increased binding affinities to important antioxidant and inflammatory proteins, suggesting that they may be able to reduce inflammation and oxidative stress. These results are reliable with earlier studies and offer a strong basis for additional experimental confirmation. By combining computational and experimental methods, new defenses against pesticide-induced toxicity may be developed, eventually leading to better public health outcomes.

Conclusion

The investigation into the combined effects of buprofezin, curcumin, and vitamin C on various biomarkers has yielded significant insights into their therapeutic potential. Previous studies have documented the individual effects of these compounds. Overall, this research focusses on the importance of exploring natural compound and AI approaches in drug design, particularly those involving natural products like curcumin and vitamin C. The synergistic effects observed in this study provide a promising basis for future in-vitro and in-vivo investigations and the development of novel treatments for diseases characterized by chronic inflammation and oxidative stress.

Limitation and future protectives

This study provides a strong basis for understanding the protective potential of curcumin and vitamin C AI drug against buprofezin-induced toxicity. However, there are some limitations, including the dependence on

AI pharmacophore	PyRx binding affinity energies (KJ/mol)	CB Dock 2 binding affinity energies (KJ/mol)
Ascorbic acid		
CAT		
1	− 7.1	− 7.4
2	− 5.3	− 5.7
3	− 6.6	− 6.7
4	− 6.7	− 6.8
5	− 5	− 5.2
6	− 6.7	− 7.0
IL-1B		
1	− 5.4	− 5.0
2	− 5.2	− 5.1
3	− 6.6	− 6.6
4	− 5.1	− 4.9
5	− 5.5	− 4.7
6	− 5.3	− 4.7
IL-6		
1	− 4.9	− 4.7
2	− 4.8	− 4.7
3	− 6.6	− 6.3
4	− 4.9	− 4.9
5	− 4.6	− 4.6
6	− 4.3	− 4.7
SOD		
1	− 4.8	− 4.6
2	− 4.7	− 4.9
3	− 5.6	− 6.1
4	− 4.8	− 4.6
5	− 4.7	− 5.1
6	− 4.6	− 4.7
TNF-alpha		
1	− 5.5	− 6.3
2	− 5.5	− 5.5
3	− 5.9	− 6.5
4	− 5.1	− 6.0
5	− 5.4	− 5.6
6	− 5.9	− 5.6
Curcumin		
CAT		
1	− 6.2	− 6.4
2	− 6.5	− 6.8
3	− 6.1	− 5.7
4	− 4.6	− 4.2
5	− 4.9	− 5.0
6	− 4.6	− 4.7
IL-1B		
1	− 6.2	− 7.0
2	− 6.5	− 7.1
3	− 7.3	− 7.5
4	− 5.6	− 6.3
5	− 5.9	− 6.1
6	− 5.7	− 6.0
IL-6		
1	− 6.7	− 7.2
2	− 6.3	− 7.1
3	− 6.8	− 7.1
Continued		

AI pharmacophore	PyRx binding affinity energies (KJ/mol)	CB Dock 2 binding affinity energies (KJ/mol)
4	− 6.2	− 6.5
5	− 6.2	− 6.4
6	− 6.0	− 6.8
SOD		
1	− 6.4	− 6.8
2	− 6.5	− 6.7
3	− 5.8	− 6.7
4	− 4.1	− 5.4
5	− 5.6	− 5.9
6	− 5.5	− 7.2
TNF-alpha		
1	− 5.9	− 7.1
2	− 5.9	− 7.0
3	− 4.9	− 6.5
4	− 5.1	− 6.6
5	− 5.4	− 6.3
6	− 5.1	− 7.0

Table 7. Comparison of binding affinity energies of all AI ligands with receptor proteins.

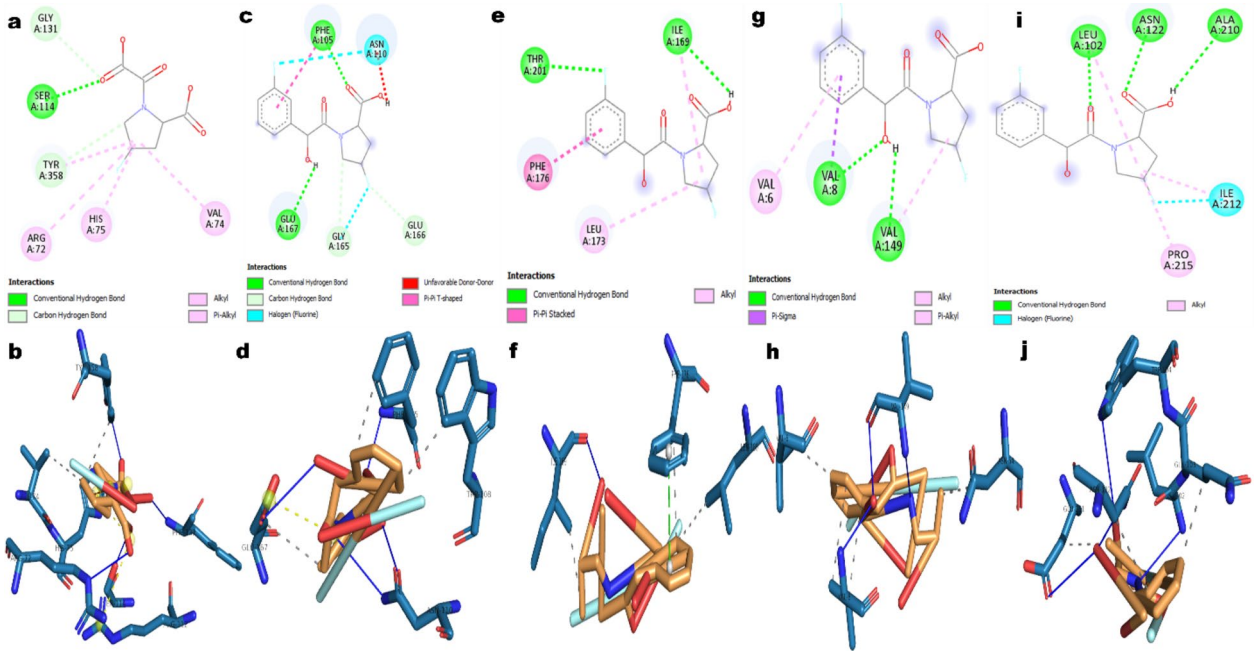

Fig. 7. 2D and 3D Molecular interactions diagrams of ascorbic acid AI ligands with receptors proteins (CAT, IL-1B, IL-6, SOD, TNF- α).

validated 3D protein models and the assumption of rigid protein structures in docking studies. While ADME predictions are promising, they need confirmation through in-vitro and in-vivo experiments.

Future research can build on these findings by validating results with experimental studies and considering protein flexibility in docking simulations for more accurate predictions. Expanding the scope to include other compounds and conducting clinical trials will further enhance therapeutic strategies. Integrating multi-omics data with computational models could also provide deeper insights into the mechanisms and improve overall treatment outcomes.

AI declaration

AI was used to improve the language and grammar of the research. The AI employed for this purpose were Grammarly and ChatGPT.

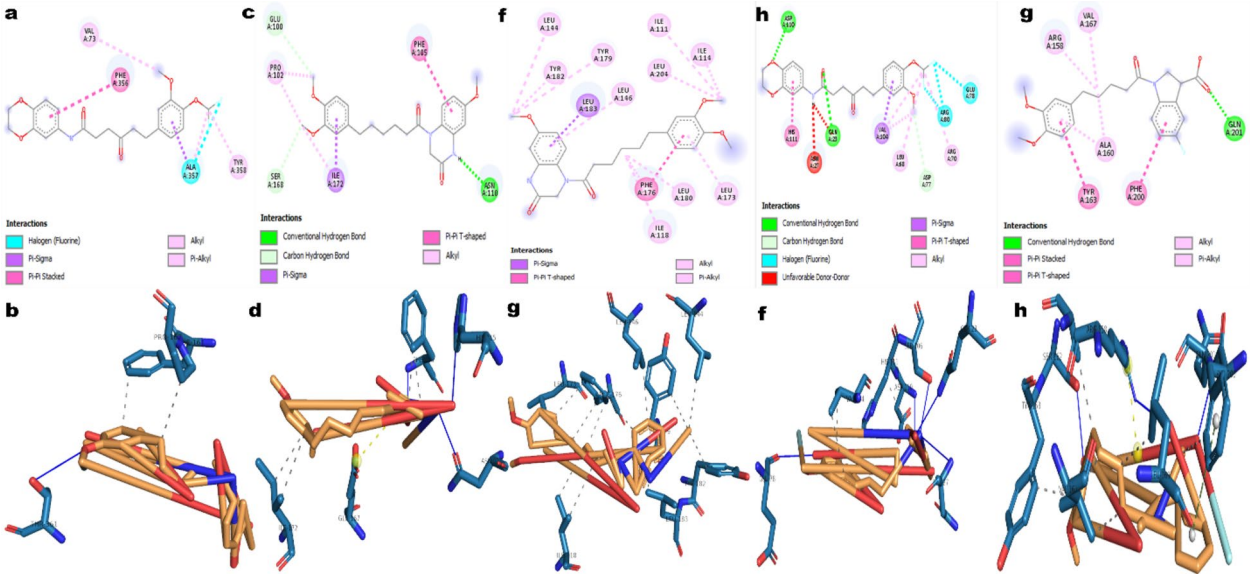

Fig. 8. 2D and 3D Molecular interactions diagrams of curcumin AI ligands with receptors proteins (CAT, IL-1B, IL-6, SOD, TNF- α).

Residues	Bond Category	Bond Type	Bond Length	Color
Ascorbic acid AI ligand 1 with Catalase (CAT)				
A:SER114:HG - N:UNL1:O	Hydrogen Bond	Conventional Hydrogen Bond	2.26	
N:UNL1:H - N:UNL1:O	Hydrogen Bond	Conventional Hydrogen Bond	2.51	
A:GLY131:CA - N:UNL1:O	Hydrogen Bond	Carbon Hydrogen Bond	3.28	
N:UNL1:C - A:TYR358:OH	Hydrogen Bond	Carbon Hydrogen Bond	3.24	
A:ARG72 - N:UNL1	Hydrophobic	Alkyl	5.03	
A:VAL74 - N:UNL1	Hydrophobic	Alkyl	5.45	
A:HIS75 - N:UNL1	Hydrophobic	Pi-Alkyl	4.71	
A:TYR358 - N:UNL1	Hydrophobic	Pi-Alkyl	4.88	
curcumin AI ligand 3 with IL-1B				
N:UNL1:H - A:ASN110:OD1	Hydrogen Bond	Conventional Hydrogen Bond	2.42754	
N:UNL1:C - A:GLU100:O	Hydrogen Bond	Carbon Hydrogen Bond	3.61412	
N:UNL1:C - A:SER168:O	Hydrogen Bond	Carbon Hydrogen Bond	3.51491	
A:ILE172:CG2 - N:UNL1	Hydrophobic	Pi-Sigma	3.95684	
A:ILE172:CD1 - N:UNL1	Hydrophobic	Pi-Sigma	3.88671	
A:PHE105 - N:UNL1	Hydrophobic	Pi-Pi T-shaped	4.76335	
N:UNL1:C - A:PRO102	Hydrophobic	Alkyl	3.92546	
N:UNL1:C - A:PRO102	Hydrophobic	Alkyl	4.80655	
N:UNL1:C - A:ILE172	Hydrophobic	Alkyl	4.26671	

Table 8. Molecular interaction details of ascorbic acid AI ligand 1 with CAT and curcumin AI ligand 3 with IL-1B.

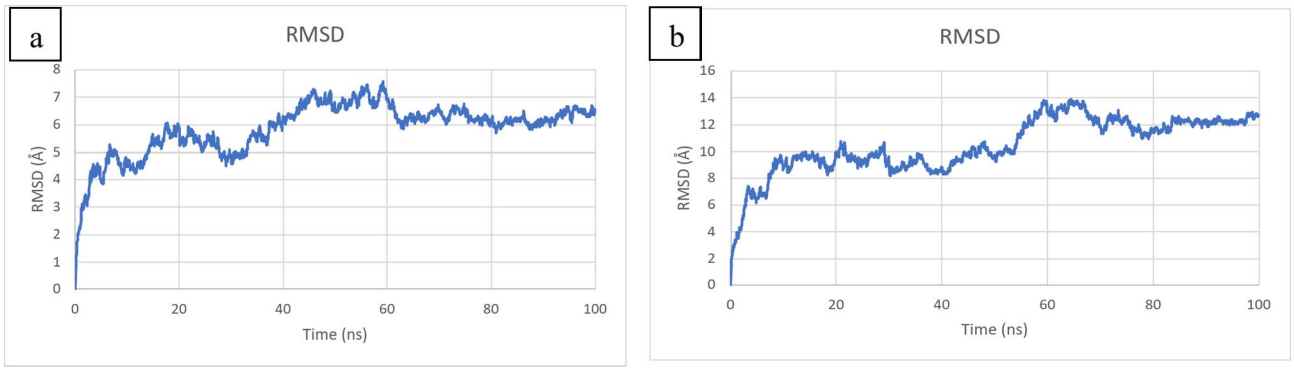

Fig. 9. RSMD graph (**a**) CAT with Ascorbic acid AI ligand 1 and (**b**) IL-1B with curcumin AI ligand 3.

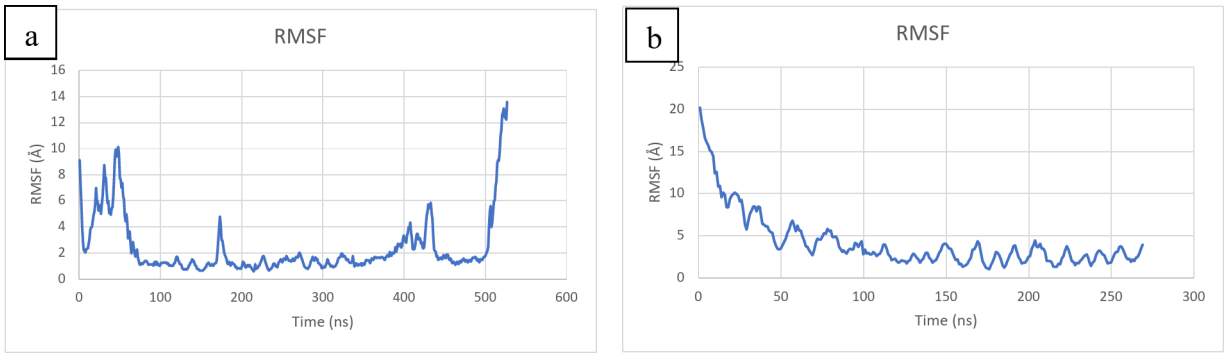

Fig. 10. RSMF graphs (**a**) CAT with Ascorbic acid AI ligand 1 and (**b**) IL-1B with curcumin AI ligand 3.

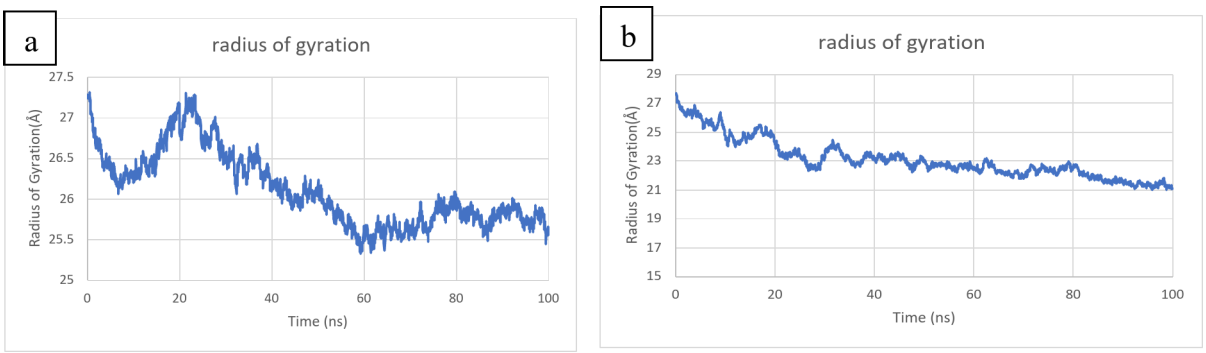

Fig. 11. Rg graphs (**a**) CAT with Ascorbic acid AI ligand 1 and (**b**) IL-1B with curcumin AI ligand 3.

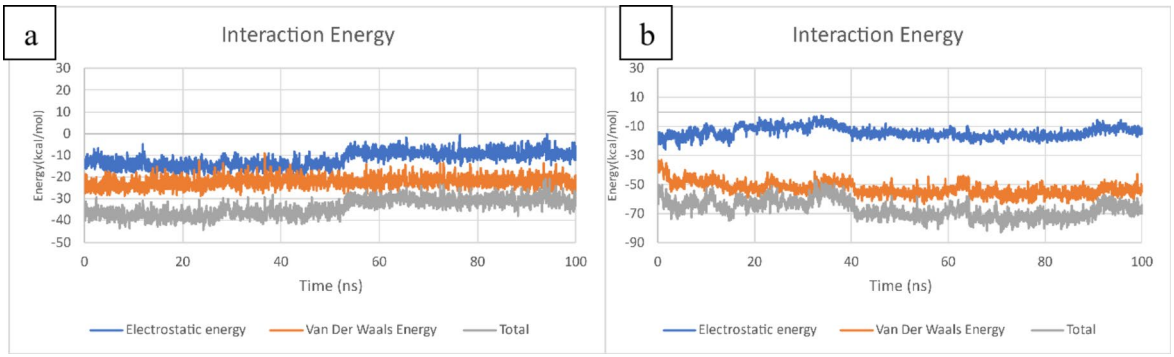

Fig. 12. Interaction energy graphs (**a**) CAT with Ascorbic acid AI ligand 1 and (**b**) IL-1B with curcumin AI ligand 3.

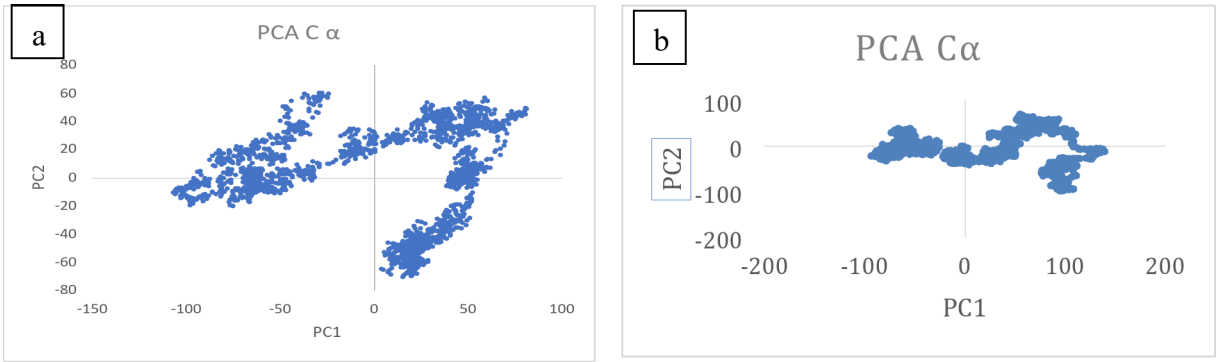

Fig. 13. PCA graphs (**a**) CAT with Ascorbic acid AI ligand 1 and (**b**) IL-1B with curcumin AI ligand.

Energy component	Average	Std. dev	Std. err. of mean
VDWAALS	− 22.8798	2.2709	0.7181
EEL	− 23.0513	4.6861	1.4819
EGB	29.5684	3.4303	1.0847
ESURF	− 3.4280	0.1588	0.0502
DELTA G gas	− 45.9311	5.0198	1.5874
DELTA G solv	26.1404	3.3575	1.0617
DELTA TOTAL	− 19.7907	2.5367	0.8022

Table 9. MMGBSA of CAT-ascorbic acid AI Ligand 1 complex.

Energy component	Average	Std. dev.	Std. err. of mean
VDWAALS	− 22.8798	2.2709	0.7181
EEL	− 23.0513	4.6861	1.4819
EPB	33.5226	4.2837	1.3546
ENPOLAR	− 17.3121	0.5998	0.1897
EDISPER	29.0066	0.7393	0.2338
DELTA G gas	− 45.9311	5.0198	1.5874
DELTA G solv	45.2170	4.6192	1.4607
DELTA TOTAL	− 0.7140	3.4670	1.0964

Table 10. MMPBSA of CAT ascorbic acid AI Ligand 1 complex.

Energy component	Average	Std. dev.	Std. err. of mean
VDWAALS	− 52.2473	4.9195	1.5557
EEL	− 26.7441	5.6438	1.7847
EGB	48.2068	4.9880	1.5773
ESURF	− 6.4227	0.4635	0.1466
DELTA G gas	− 78.9914	7.0064	2.2156
DELTA G solv	41.7841	4.8516	1.5342
DELTA TOTAL	− 37.2074	5.0900	1.6096

Table 11. MMGBSA of IL-1B curcumin AI Ligand 3 complex.

Energy component	Average	Std. dev.	Std. err. of mean
VDWAALS	− 52.2473	4.9195	1.5557
EEL	− 26.7441	5.6438	1.7847
EPB	53.8040	5.2211	1.6511
ENPOLAR	− 37.3801	3.0600	0.9677
EDISPER	63.6371	3.4446	1.0893
DELTA G gas	− 78.9914	7.0064	2.2156
DELTA G solv	80.0610	4.3437	1.3736
DELTA TOTAL	1.0696	6.6186	2.0930

Table 12. MMPBSA of IL-1B curcumin AI Ligand 3 complex.

AI ligand	TPSA (Å^2)	Lipophilicity log Po/w	Water solubility	GI absorption	BBB permeant	Lipinski voilation
Ascorbic acid						
1	94.91	− 0.55	Soluble	High	No	No
2	98.07	− 1.04	Soluble	High	No	No
3	77.84	1.08	Soluble	High	No	No
4	77.84	− 0.13	Soluble	High	No	No
5	104.14	− 1.23	Soluble	High	No	No
6	77.84	− 0.5	Soluble	High	No	No
Curcumin						
1	76.07	3.42	Moderately soluble	High	Yes	No
2	83.09	3.41	Poorly soluble	High	No	No
3	77.10	3.26	Poorly soluble	High	Yes	No
4	53.99	4.79	Poorly soluble	High	Yes	No
5	74.22	3.95	Poorly soluble	High	Yes	No
6	66.02	4.01	Poorly soluble	High	Yes	No

Table 13. The ADME properties of ascorbic acid and curcumin AI ligands.

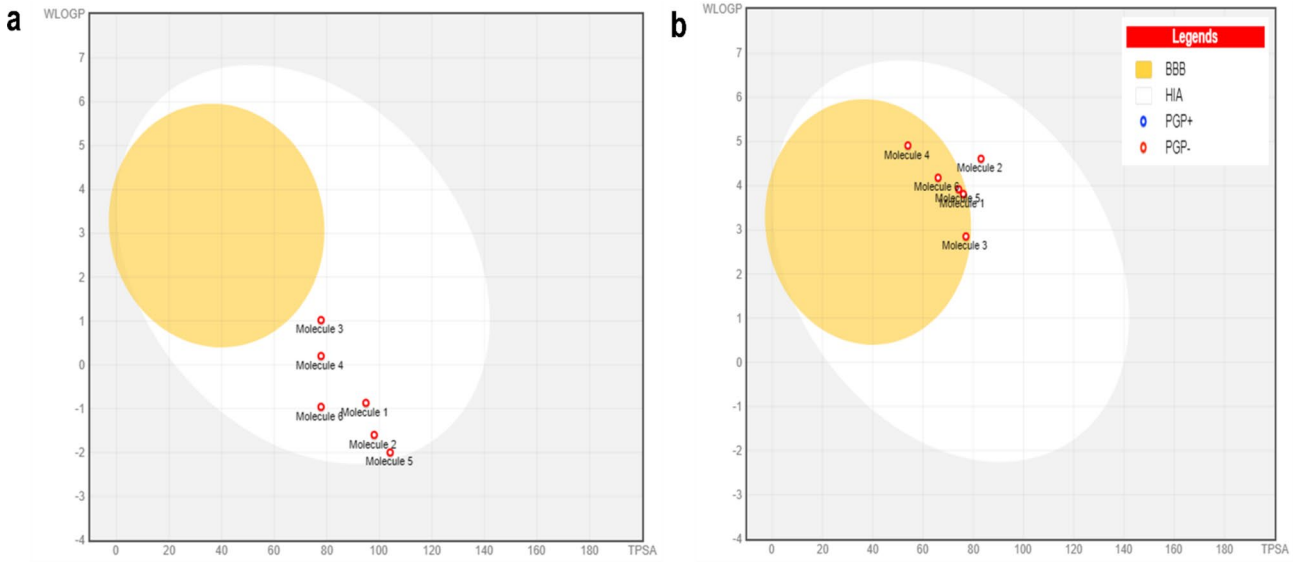

Fig. 14. Boiled egg diagram of (**a**) Ascorbic acid AI ligands (**b**) Curcumin AI ligands. The white region of the egg represents the GI absorption and yellow yolk of the egg represents the Blood Brain Barrier crossing.

Property name	Predicted value	Property unit	Predictive confidence	Is prediction within training range?	Is MW within training range?
Ascorbic acid AI ligand 1					
AMES mutagenesis	Safe	Category (toxic/safe)	0	–	Yes
Avian	Safe	Category (toxic/safe)	0.006	–	Yes
Bee	Toxic	Category (toxic/safe)	0.711	–	Yes
Bioconcentration factor	-0.15	log10(L/kg)	-	Yes	Yes
Biodegradation	Toxic	Category (toxic/safe)	0.943	–	Yes
Carcinogenesis	Safe	Category (toxic/safe)	0.017	–	Yes
Crustacean	Safe	Category (toxic/safe)	0.006	–	Yes
Liver injury I	Safe	Category (toxic/safe)	0.26	–	Yes
Eye corrosion	Safe	Category (toxic/safe)	0.199	–	Yes
Eye irritation	Toxic	Category (toxic/safe)	0.937	–	Yes
Maximum tolerated dose	0.73	log mg/kg/day	-	Yes	Yes
Liver injury II	Toxic	Category (toxic/safe)	0.617	–	Yes
hERG blockers	Safe	Category (toxic/safe)	0.003	–	Yes
Daphnia maga	5.45	−log10[(mg/L)/(1000*MW)]	-	Yes	Yes
Micronucleos	Toxic	Category (toxic/safe)	0.881	–	Yes
NR-AhR	Safe	Category (toxic/safe)	0	–	Yes
NR-AR	Safe	Category (toxic/safe)	0.004	–	Yes
NR-AR-LBD	Safe	Category (toxic/safe)	0.03	–	Yes
NR-aromatase	Safe	Category (toxic/safe)	0	–	Yes
NR-ER	Safe	Category (toxic/safe)	0.023	–	Yes
NR-ER-LBD	Safe	Category (toxic/safe)	0	–	Yes
NR-GR	Safe	Category (toxic/safe)	0.004	–	Yes
NR-PPAR-gamma	Safe	Category (toxic/safe)	0	–	Yes
NR-TR	Safe	Category (toxic/safe)	0	–	Yes
T. pyriformis	5.46	−log10[(mg/L)/(1000*MW)]	-	Yes	Yes
Rat (acute)	1.91	mol/kg	-	Yes	Yes
Rat (chronic oral)	1.95	LOAEL	-	Yes	Yes
Fathead minnow	3.52	−log10[(mg/L)/(1000*MW)]	-	Yes	Yes
Respiratory disease	Safe	Category (toxic/safe)	0.322	–	Yes
Skin sensitisation	Toxic	Category (toxic/safe)	0.555	–	Yes
SR-ARE	Safe	Category (toxic/safe)	0.035	–	Yes
SR-ATAD5	Safe	Category (toxic/safe)	0	–	Yes
SR-HSE	Safe	Category (toxic/safe)	0.003	–	Yes
SR-MMP	Safe	Category (toxic/safe)	0	–	Yes
SR-p53	Safe	Category (toxic/safe)	0	–	Yes
Curcumin AI ligand 3					
AMES mutagenesis	Safe	Category (toxic/safe)	0.005	–	Yes
Avian	Safe	Category (toxic/safe)	0.035	–	Yes
Bee	Toxic	Category (toxic/safe)	0.775	–	Yes
Bioconcentration factor	0.71	log10(L/kg)	-	Yes	Yes
Biodegradation	Safe	Category (toxic/safe)	0.023	–	Yes
Carcinogenesis	Safe	Category (toxic/safe)	0.201	–	Yes
Crustacean	Toxic	Category (toxic/safe)	0.824	–	Yes
Liver injury I	Toxic	Category (toxic/safe)	0.528	–	Yes
Eye corrosion	Safe	Category (toxic/safe)	0	–	Yes
Eye irritation	Safe	Category (toxic/safe)	0.028	–	Yes
Maximum tolerated dose	0.74	log mg/kg/day	-	Yes	Yes
Liver injury II	Toxic	Category (toxic/safe)	0.682	–	Yes
hERG blockers	Toxic	Category (toxic/safe)	0.954	–	Yes
Daphnia maga	5.47	−log10[(mg/L)/(1000*MW)]	-	Yes	Yes
Micronucleos	Toxic	Category (toxic/safe)	0.665	–	Yes
NR-AhR	Toxic	Category (toxic/safe)	0.511	–	Yes
NR-AR	Safe	Category (toxic/safe)	0.048	–	Yes
NR-AR-LBD	Safe	Category (toxic/safe)	0.006	–	Yes
NR-aromatase	Safe	Category (toxic/safe)	0.003	–	Yes
Continued					

Property name	Predicted value	Property unit	Predictive confidence	Is prediction within training range?	Is MW within training range?
NR-ER	Safe	Category (toxic/safe)	0.085	–	Yes
NR-ER-LBD	Safe	Category (toxic/safe)	0	–	Yes
NR-GR	Toxic	Category (toxic/safe)	0.508	–	Yes
NR-PPAR-gamma	Safe	Category (toxic/safe)	0.012	–	Yes
NR-TR	Safe	Category (toxic/safe)	0.225	–	Yes
T. pyriformis	-28.72	−log10[(mg/L)/(1000*MW)]	-	No	Yes
Rat (acute)	2.05	mol/kg	-	Yes	Yes
Rat (chronic oral)	2.14	LOAEL	-	Yes	Yes
Fathead minnow	4.72	−log10[(mg/L)/(1000*MW)]	-	Yes	Yes
Respiratory disease	Safe	Category (toxic/safe)	0.144	–	Yes
Skin sensitisation	Safe	Category (toxic/safe)	0.376	–	Yes
SR-ARE	Toxic	Category (toxic/safe)	0.852	–	Yes
SR-ATAD5	Safe	Category (toxic/safe)	0.22	–	Yes
SR-HSE	Safe	Category (toxic/safe)	0.085	–	Yes
SR-MMP	Toxic	Category (toxic/safe)	0.59	–	Yes
SR-p53	Safe	Category (toxic/safe)	0	–	Yes

Table 14. .

Data availability

All the data generated in this research work has been included in this manuscript.

Received: 29 August 2024; Accepted: 7 November 2024
Published online: 18 November 2024

References

1. Ji, X. et al. Potential hepatic toxicity of buprofezin at sublethal concentrations: ROS-mediated conversion of energy metabolism. *J. Hazard. Mater.* **320**, 176–186 (2016).
2. Iqbal, M. J. et al. Interplay of oxidative stress, cellular communication and signaling pathways in cancer. *Cell. Communication Signal.* **22**(1), 7 (2024).
3. Bakchi, B. et al. An overview on applications of SwissADME web tool in the design and development of anticancer, antitubercular and antimicrobial agents: a medicinal chemist's perspective. *J. Mol. Struct.* **1259**, 132712 (2022).
4. Ghazanfar, M., Shahid, S. & Qureshi, I. Z. Vitamin C attenuates biochemical and genotoxic damage in common carp (Cyprinus carpio) upon joint exposure to combined toxic doses of fipronil and buprofezin insecticides. *Aquat. Toxicol.* **196**, 43–52 (2018).
5. Popko, K. et al. Proinflammatory cytokines Il-6 and TNF-α and the development of inflammation in obese subjects. *Eur. J. Med. Res.* **15**, 1–3 (2010).
6. Carlson, N. G. et al. Inflammatory cytokines IL-1α, IL-1β, IL-6, and TNF-α impart neuroprotection to an excitotoxin through distinct pathways. *J. Immunol.* **163**(7), 3963–3968 (1999).
7. Blanco-Gonzalez, A. et al. The role of AI in drug discovery: challenges, opportunities, and strategies. *Pharmaceuticals*. **16**(6), 891 (2023).
8. Jiménez-Luna, J. et al. Artificial intelligence in drug discovery: recent advances and future perspectives. *Expert Opin. Drug Discov.* **16**(9), 949–959 (2021).
9. Naveed, M. et al. Artificial intelligence assisted pharmacophore design for philadelphia chromosome-positive leukemia with gamma-tocotrienol: a toxicity comparison approach with asciminib. *Biomedicines*. **11**(4), 1041 (2023).
10. Geer, L. Y. et al. The NCBI biosystems database. *Nucleic Acids Res.* **38**(suppl_1), D492–D496 (2010).
11. Bienert, S. et al. The SWISS-MODEL Repository—new features and functionality. *Nucleic Acids Res.* **45**(D1), D313–D319 (2017).
12. Hollingsworth, S. A. & Karplus, P. A. A fresh look at the Ramachandran plot and the occurrence of standard structures in proteins. (2010).
13. Colovos, C. & Yeates, T. O. Verification of protein structures: patterns of nonbonded atomic interactions. *Protein Sci.* **2**(9), 1511–1519 (1993).
14. Kim, S. et al. PubChem substance and compound databases. *Nucleic Acids Res.* **44**(D1), D1202–D1213 (2016).
15. Bai, Q. et al. WADDAICA: a webserver for aiding protein drug design by artificial intelligence and classical algorithm. *Comput. Struct. Biotechnol. J.* **19**, 3573–3579 (2021).
16. Koes, D. R. The Pharmit backend: a computer systems approach to enabling interactive online drug discovery. *IBM J. Res. Dev.* **62**(6), 1–3 (2018).
17. Naveed, M. et al. Assessment of Melia azedarach plant extracts activity against hypothetical protein of mycobacterium tuberculosis via GC-MS analysis and in-silico approaches. *J. Comput. Biophys. Chem.* **23**(3), 299–320 (2024).
18. Dallakyan, S. & Olson, A. J. Small-molecule library screening by docking with PyRx. *Chem. Biol. Methods Protocols*. 243–250 (2015).
19. Naveed, M. et al. The natural breakthrough: phytochemicals as potent therapeutic agents against spinocerebellar ataxia type 3. *Sci. Rep.* **14**(1), 1529 (2024).
20. Liu, Y. et al. CB-Dock2: improved protein–ligand blind docking by integrating cavity detection, docking and homologous template fitting. *Nucleic Acids Res.* **50**(W1), W159–W164 (2022).
21. Adasme, M. F. et al. PLIP 2021: expanding the scope of the protein–ligand interaction profiler to DNA and RNA. *Nucleic Acids Res.* **49**(W1), W530–W534 (2021).
22. Yuan, S., Chan, H. S. & Hu, Z. Using PyMOL as a platform for computational drug design. *Wiley Interdiscip. Rev. Comput. Mol. Sci.* **7**(2), e1298 (2017).
23. Tian, C. *Improving the Accuracy of Amber Force Field for Biomolecular Simulation* (State University of New York at Stony Brook, 2019).

24. Mark, P. & Nilsson, L. Structure and dynamics of the TIP3P, SPC, and SPC/E water models at 298 K. *J. Phys. Chem. A*. **105**(43), 9954–9960 (2001).
25. Zaheer, M. et al. Uncovering the impact of SARS-CoV2 spike protein variants on human receptors: a molecular dynamics docking and simulation approach. *J. Infect. Public Health*. **16**(10), 1544–1555 (2023).
26. Wang, E. et al. End-point binding free energy calculation with MM/PBSA and MM/GBSA: strategies and applications in drug design. *Chem. Rev.* **119**(16), 9478–9508 (2019).
27. Myung, Y., de Sá, A. G. & Ascher, D. B. Deep-PK: deep learning for small molecule pharmacokinetic and toxicity prediction. *Nucleic Acids Res.* gkae254 (2024).
28. Marimuthu, K. et al. Toxicity of buprofezin on the survival of embryo and larvae of African catfish, Clarias gariepinus (Bloch). *PloS One*. **8**(10), e75545 (2013).
29. Shehzad, A., Rehman, G. & Lee, Y. S. Curcumin in inflammatory diseases. *Biofactors*. **39**(1), 69–77 (2013).
30. Chen, L. et al. A novel combination of vitamin C, curcumin and glycyrrhizic acid potentially regulates immune and inflammatory response associated with coronavirus infections: a perspective from system biology analysis. *Nutrients*. **12**(4), 1193 (2020).
31. Hatcher, H. C., Torti, F. M. & Torti, S. V. Curcumin, oxidative stress, and cancer therapy. *Oxid. Stress Cancer Biol. Ther.* 233–256 (2012).
32. Ma, C. et al. Thyroid-associated ophthalmopathy: the role of oxidative stress. *Front. Endocrinol.* **15**, 1400869 (2024).
33. Njus, D. et al. Ascorbic acid: the chemistry underlying its antioxidant properties. *Free Radic. Biol. Med.* **159**, 37–43 (2020).
34. Sunil Kumar, B., Singh, S. & Verma, R. Anticancer potential of dietary vitamin D and ascorbic acid: a review. *Crit. Rev. Food Sci. Nutr.* **57**(12), 2623–2635 (2017).
35. Nagarajan, N. et al. Application of computational biology and artificial intelligence technologies in cancer precision drug discovery. *Biomed. Res. Int.* **2019**(1), 8427042 (2019).

Acknowledgements

The authors extend their appreciation to the Research Supporting Project (RSPD2024R568), King Saud University Riyadh Saudi Arabia,

Author contributions

Conceptualization, Irfan Zia Qureshi.; Methodology, Haleema Sadia; software, Muhammad Naveed.; Validation, Haleema Sadia.; Formal analysis, Tariq Aziz.; Investigation, Muhammad Naveed; Resources, Irfan Zia Qureshi.; Data curation, Muhammad Naveed.; Writing—original draft preparation, Haleema Sadia.; Writing—review and editing, Metab Alharbi and Abdullah F Alasmari.; Visualization, Tariq Aziz.; Supervision, Irfan Zia Qureshi.; Project Administration, Thamer H Alebkairi.; Funding acquisition, Irfan Zia Qureshi.

Funding

This research did not receive any specific grant from funding agencies in the public, commercial, or not-for-profit sector except the University Research Fund, URF-2021. We are thankful to the Department of Zoology, Quaid-i-Azam University Islamabad for providing basic laboratory facilities.

Declarations

Competing interests

The authors declare no competing interests.

Additional information

Correspondence and requests for materials should be addressed to I.Z.Q. or T.A.

Reprints and permissions information is available at www.nature.com/reprints.

Publisher's note Springer Nature remains neutral with regard to jurisdictional claims in published maps and institutional affiliations.

Open Access This article is licensed under a Creative Commons Attribution-NonCommercial-NoDerivatives 4.0 International License, which permits any non-commercial use, sharing, distribution and reproduction in any medium or format, as long as you give appropriate credit to the original author(s) and the source, provide a link to the Creative Commons licence, and indicate if you modified the licensed material. You do not have permission under this licence to share adapted material derived from this article or parts of it. The images or other third party material in this article are included in the article's Creative Commons licence, unless indicated otherwise in a credit line to the material. If material is not included in the article's Creative Commons licence and your intended use is not permitted by statutory regulation or exceeds the permitted use, you will need to obtain permission directly from the copyright holder. To view a copy of this licence, visit http://creativecommons.org/licenses/by-nc-nd/4.0/.

© The Author(s) 2024